



# Monte Carlo evaluation of the $\beta^+$ signal in J-PET detector for hadrontherapy range monitoring application

A. Ruciński<sup>1</sup>, J. Baran<sup>1</sup>, J. Gajewski<sup>1</sup>, M. Garbacz<sup>1</sup>, M. Pawlik-Niedźwiecka<sup>1,2</sup>, P. Moskal<sup>2</sup>

On behalf of the J-PET collaboration

<sup>1</sup> Institute of Nuclear Physics Polish Academy of Sciences, Krakow, Poland

<sup>2</sup> Faculty of Physics, Astronomy and Applied Computer Science, Jagiellonian University, Kraków, Poland

## OBJECTIVE

### Plastic-scintillator based PET detector

Proton beam therapy (PBT) range monitoring is required to fully exploit the advantages of proton beam in the clinic. In PBT the distribution of  $\beta^+$  emitters induced by a proton beam in patient can be detected by PET scanners, the emission distribution can be reconstructed and used for monitoring of the beam range.

**The aim of this work is to study a feasibility of the J-PET technology for range verification in PBT.**

## IFJ PAN KRAKÓW

### Krakow proton beam therapy centre

- Head and neck cancer patients treatment from Oct 2016
- ~200 patients treated in two Gantry rooms
- Eye treatment from 2010
- Proteus C-235 cyclotron
- Pencil beam scanning
- Eclipse TPS
- Dedicated QA protocols



## MATERIALS AND METHODS

### Plastic-scintillator based PET detector



Fig. 1.

2<sup>nd</sup> generation modular J-PET

A prototype of a diagnostic strip-based whole body PET scanner (J-PET) has been developed and tested at the Jagiellonian University in Krakow. [1] The advantages of the system over commercial PET scanners is that it increases the geometrical acceptance and facilitates integration in the treatment room, off-line or in the treatment position. A single detection module of the modular, 2<sup>nd</sup> generation strip-PET scanner (see Fig. 1) is constructed out of thirteen 50-cm long organic scintillator strips. The light pulses produced in a strip by gamma quanta are propagated to its edges and converted into electrical signals by silicon photomultipliers (see Fig. 2). They are read-out by fast on-board front-end electronics allowing excellent overall coincidence resolving time (CRT) of about 400 ps, which shows a significant improvement compared to the standard LSO-based PET scanners.

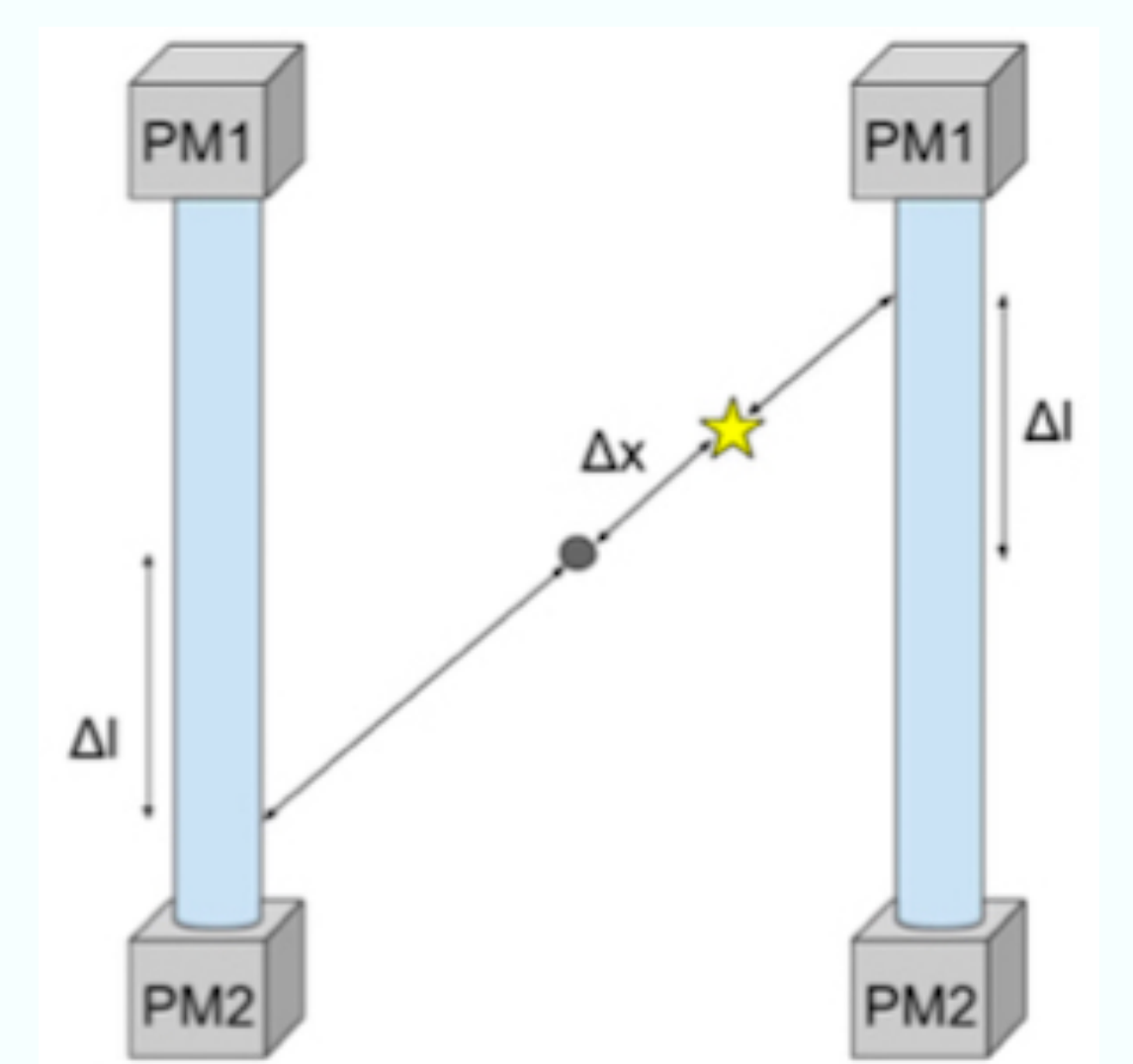


Fig. 2

### Monte Carlo simulations

GATE Monte Carlo (MC) toolkit has been used to investigate the modular JPET system efficiency for detection of  $\beta^+$  annihilation back to back photons induced in PMMA target by a proton beam (see Fig. 3). Three barrel and three dual-head configurations (see Fig. 4; re-printed from [2]) of the modular system were investigated:

- a single layer consisting of 24 modules (barrel)
- a two layer consisting of 20 and 24 modules (barrel)
- a three layers consisting of 20, 24 and 28 modules (barrel)
- a single layer consisting of 10 modules (dual-head)
- a two layer consisting of 20 and 24 modules (dual-head)
- a three layers consisting of 20, 24 and 28 modules (dual-head)

Fig. 3

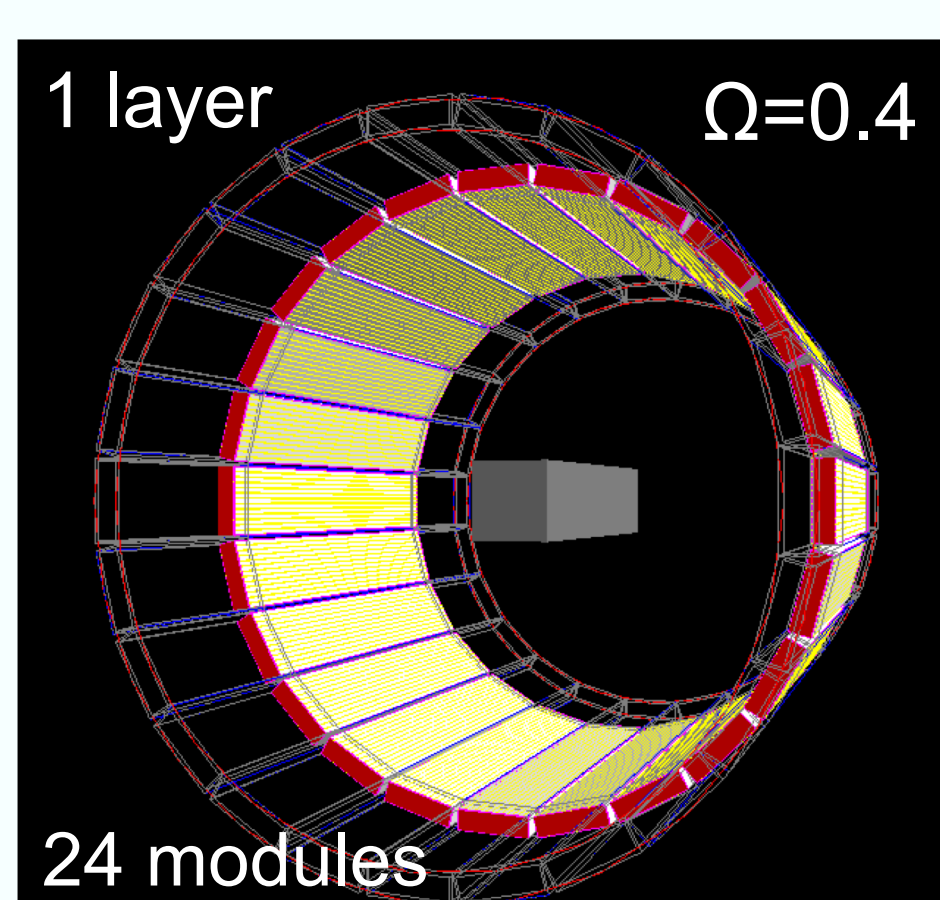
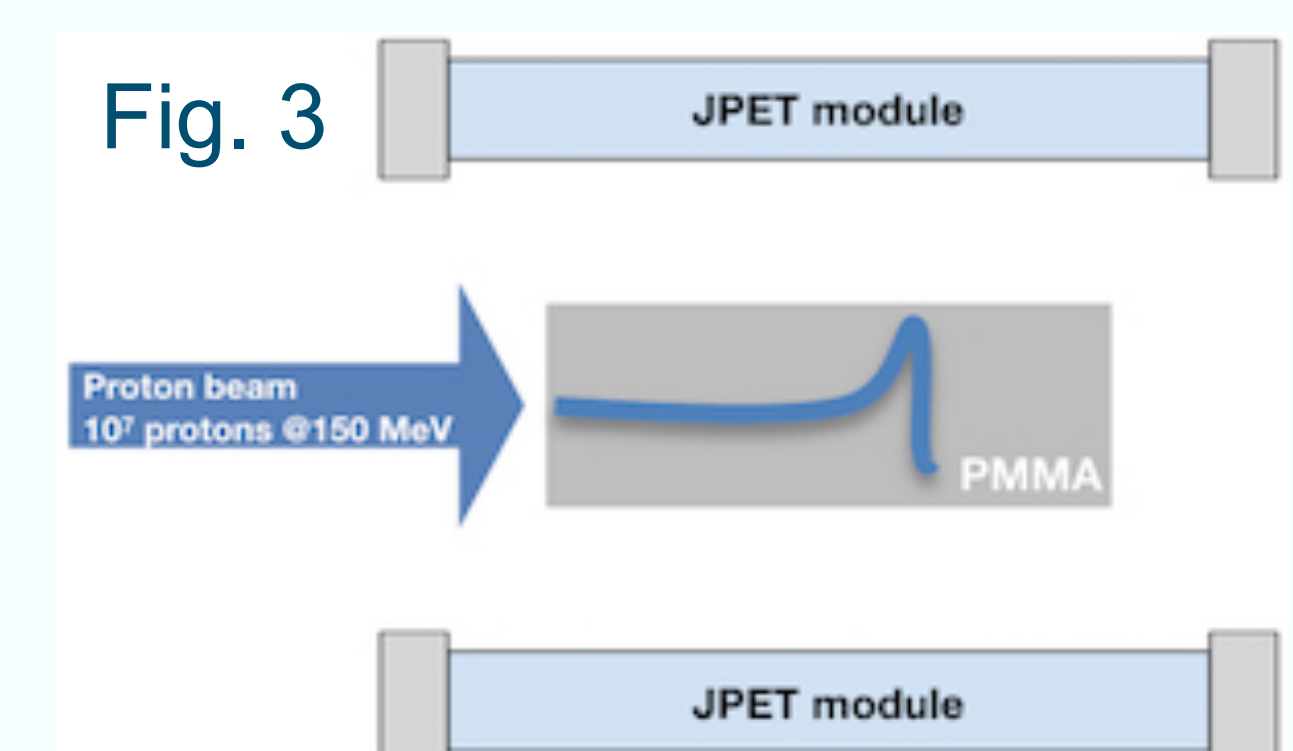


Fig. 4 (a)

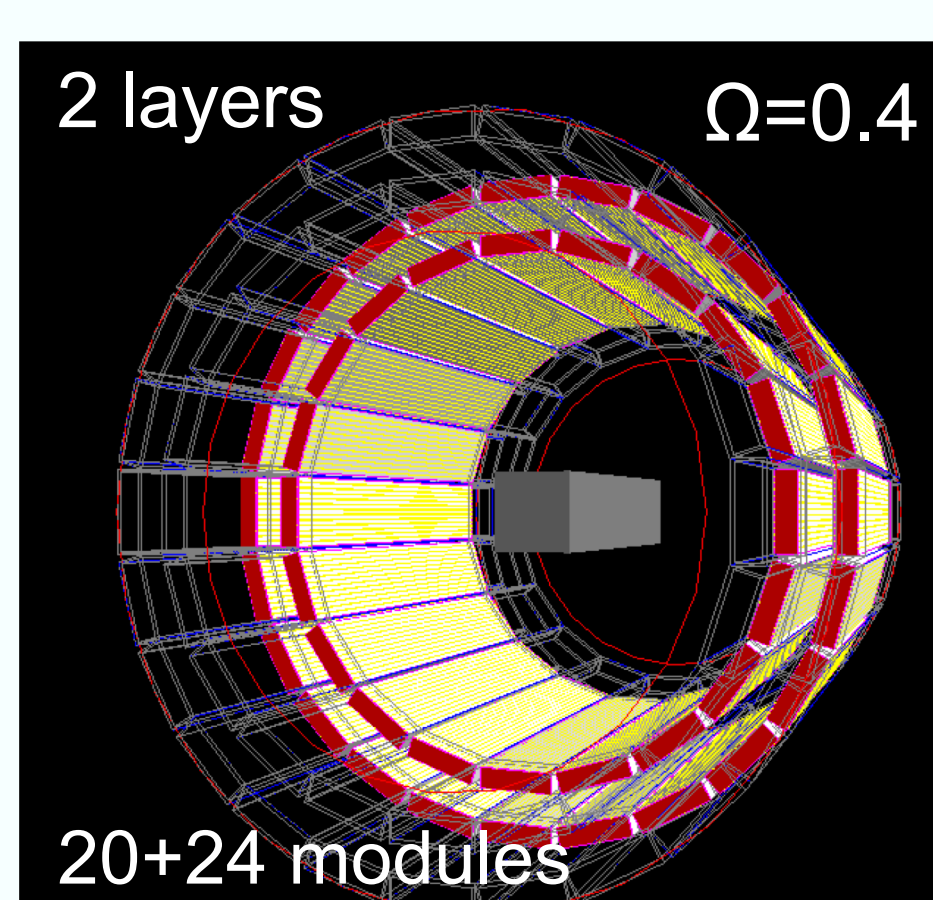


Fig. 4 (b)

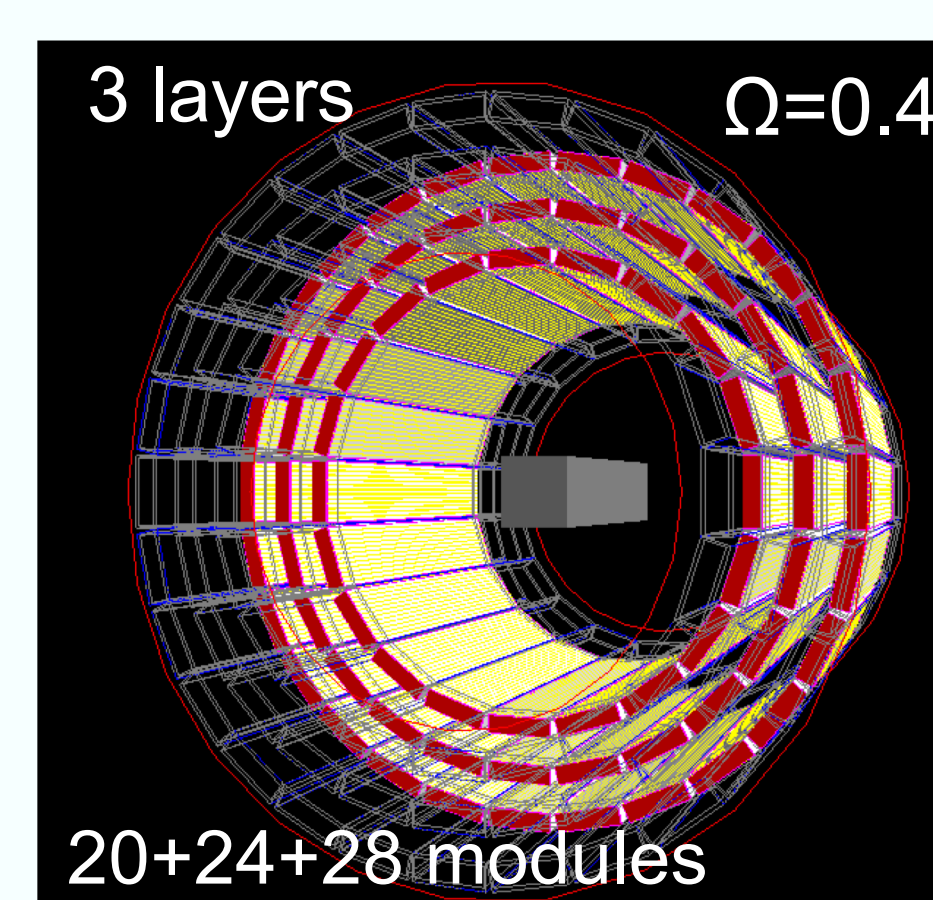


Fig. 4 (c)

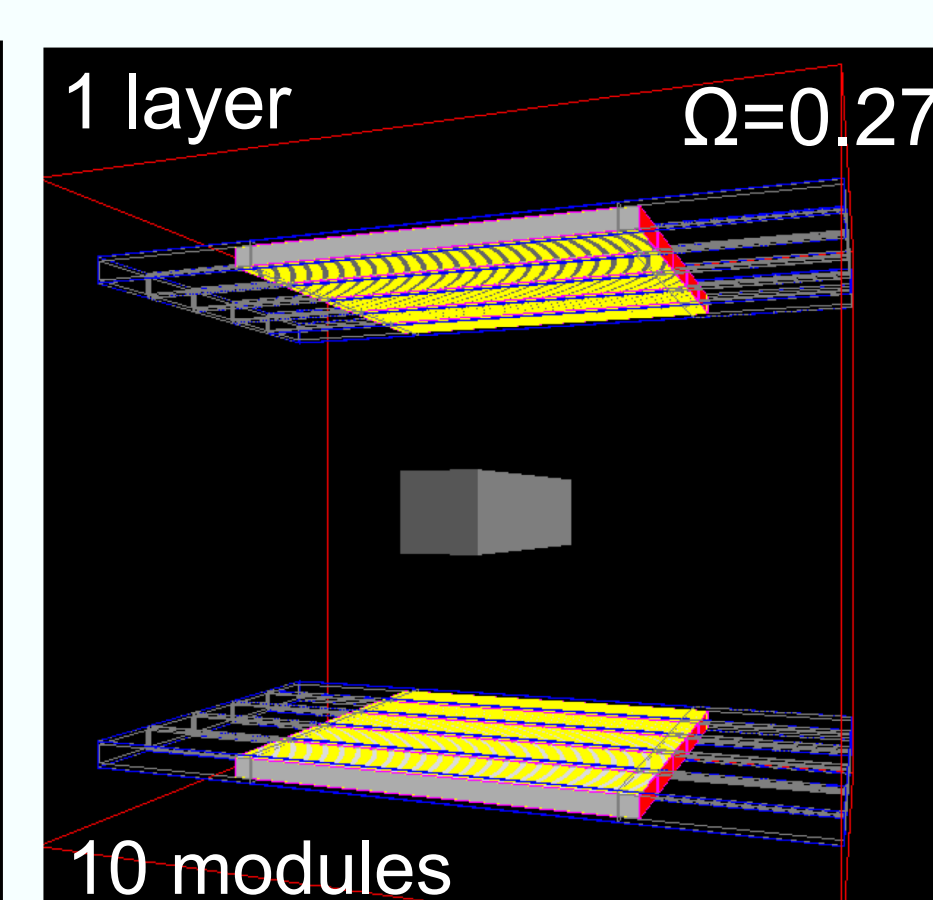


Fig. 4 (d)

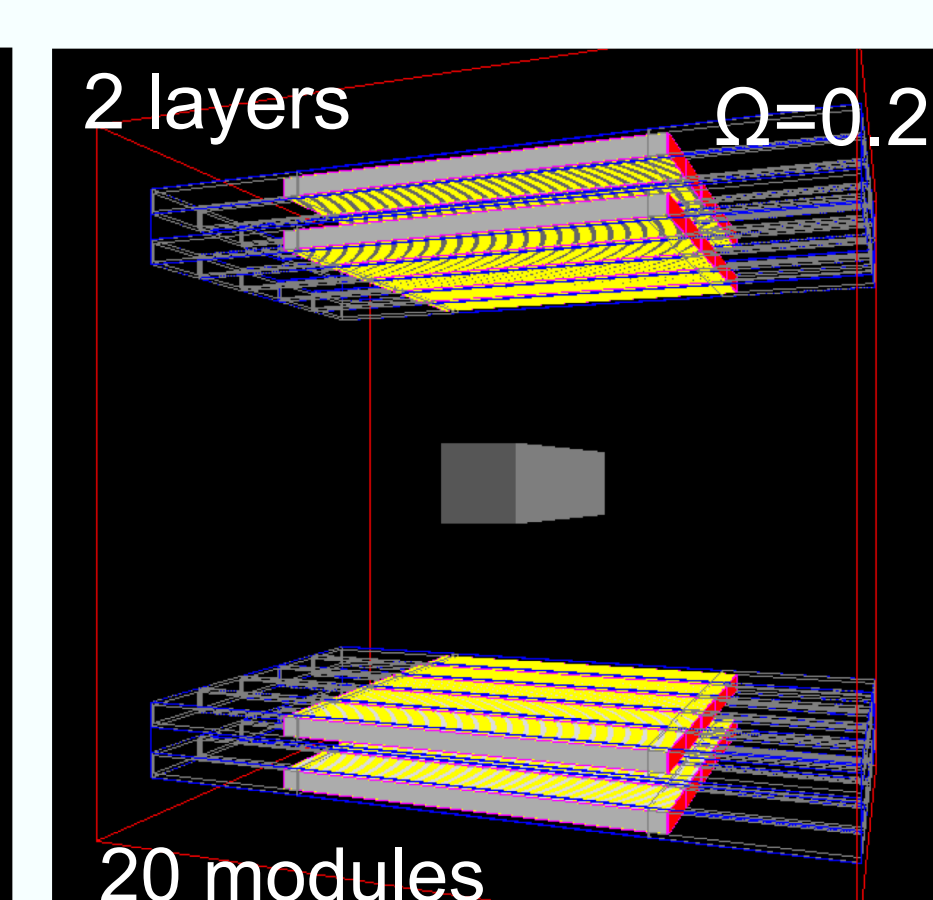


Fig. 4 (e)

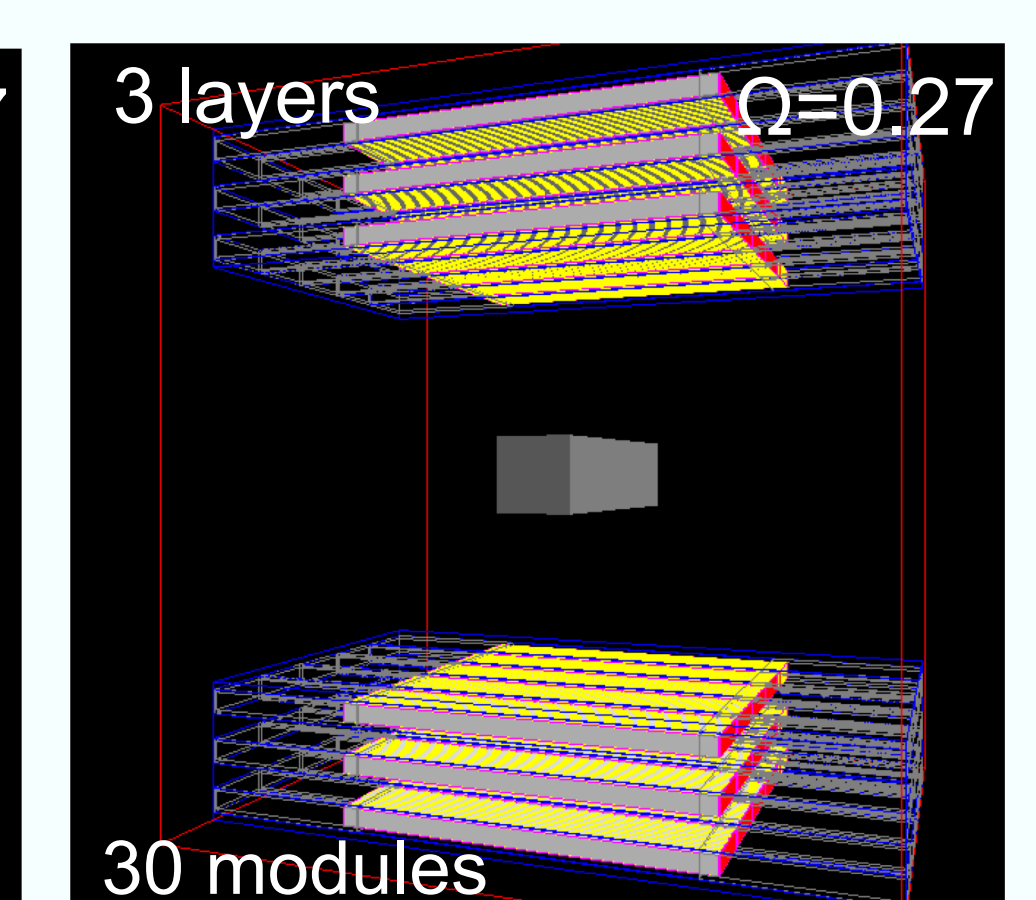


Fig. 4 (f)

## RESULTS and CONCLUSION

The activity profile as a function of depth along the beam axis built from the transversally integrated signal along the phantom (blue) compared with the dose deposition profile (red; see Fig. 5; re-printed from [2]). The detection efficiency of the strips is about 10%. The efficiency of the system in the proton beam simulation increases quadratically with the number of detector layers. It ranges from 0.14% for single layer setup to 0.95% for three layers setup. **Performed simulations suggest the signal obtained with the J-PET detector technology during proton beam therapy is sufficient for range monitoring. The results revealed that inter-spill beam range monitoring is achievable with both, dual-head and multi-layer JPET configurations. Experimental verification of the performed simulations is planned.**

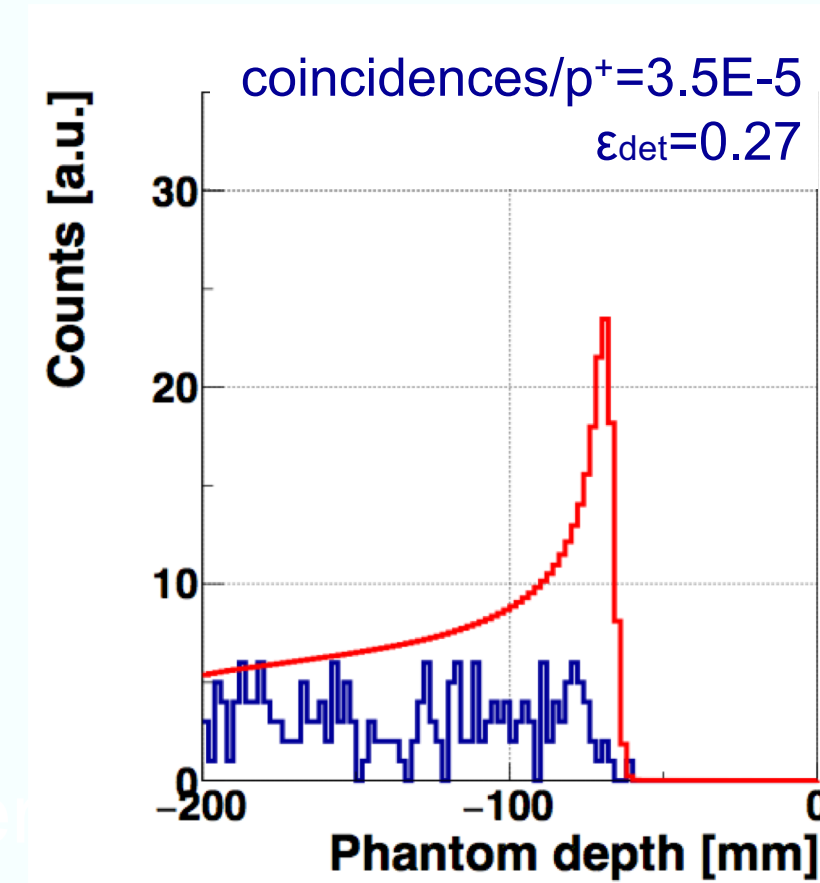


Fig. 5 (a)

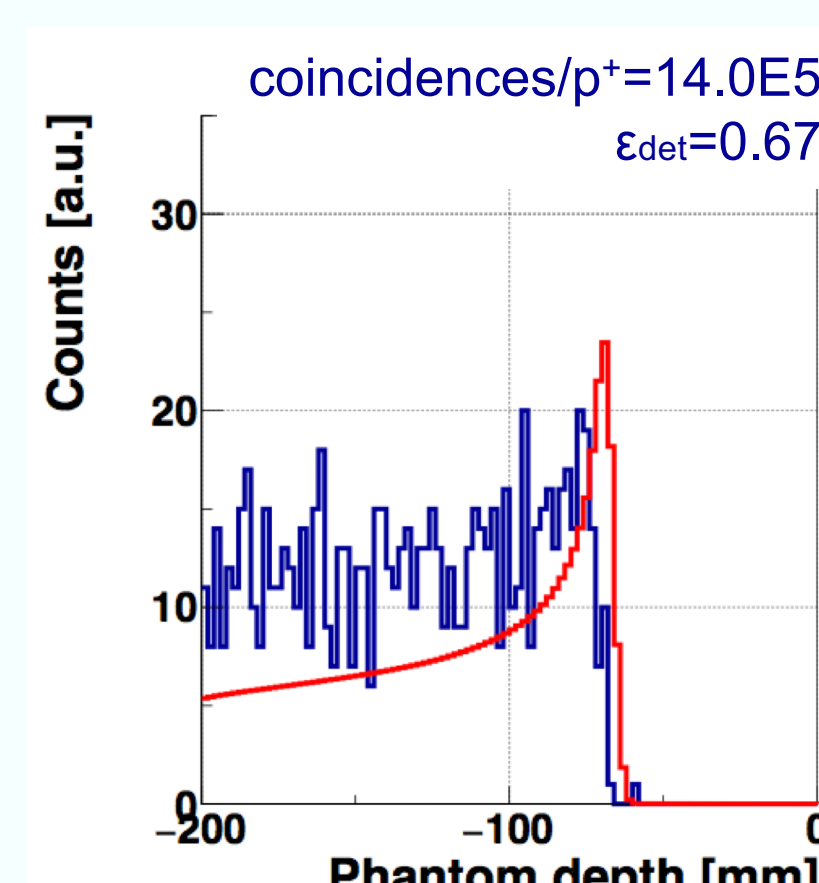


Fig. 5 (b)

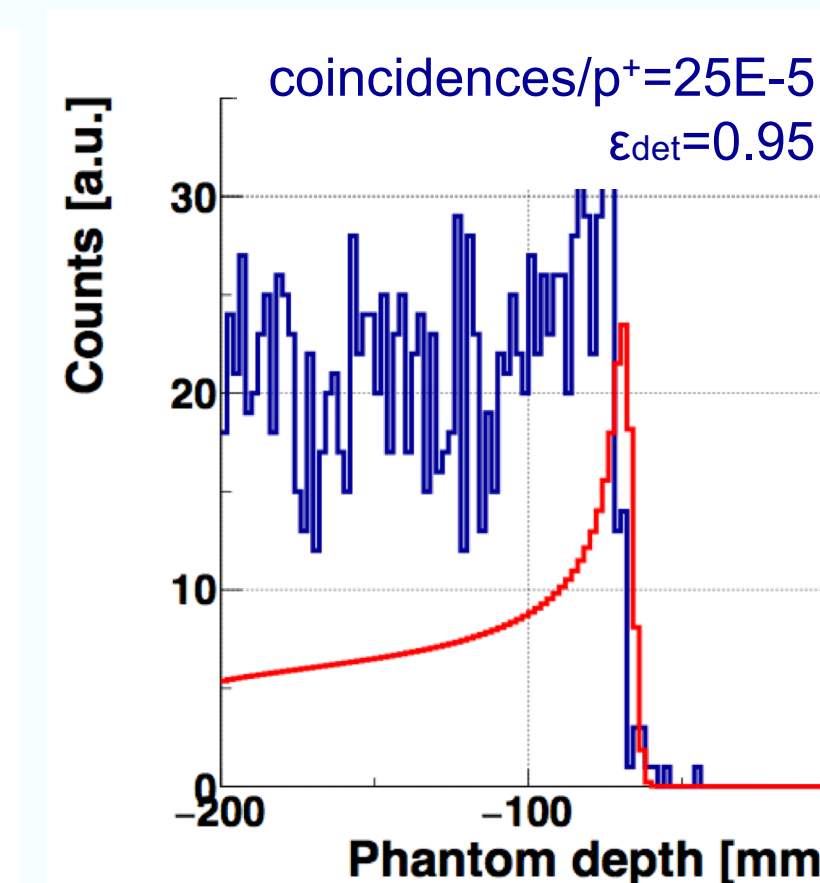


Fig. 5 (c)

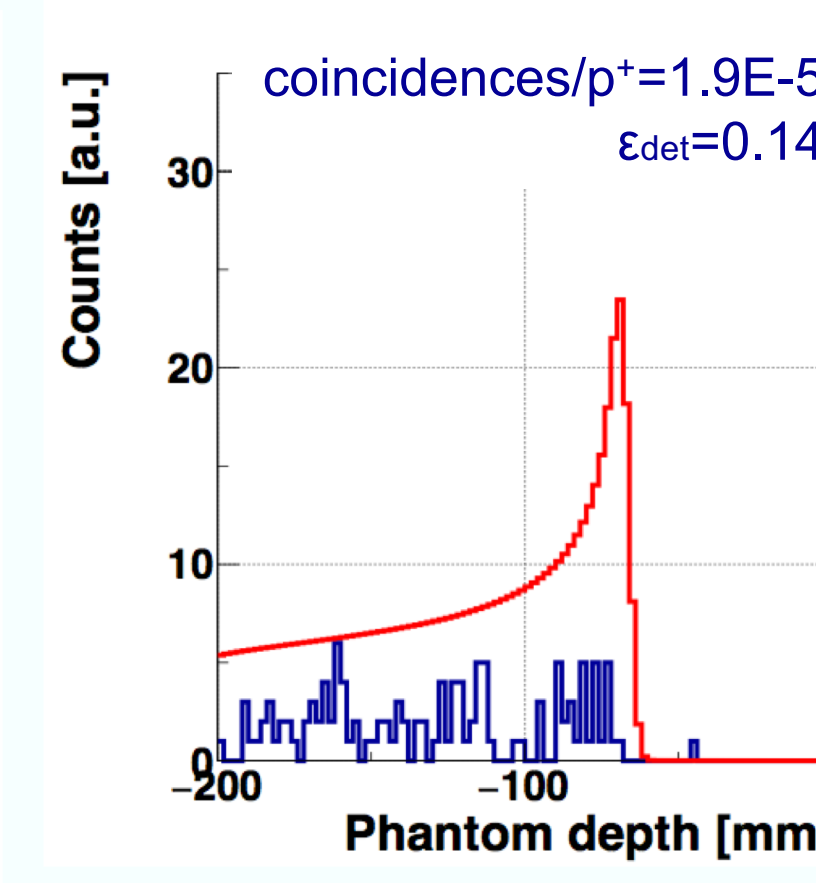


Fig. 5 (d)

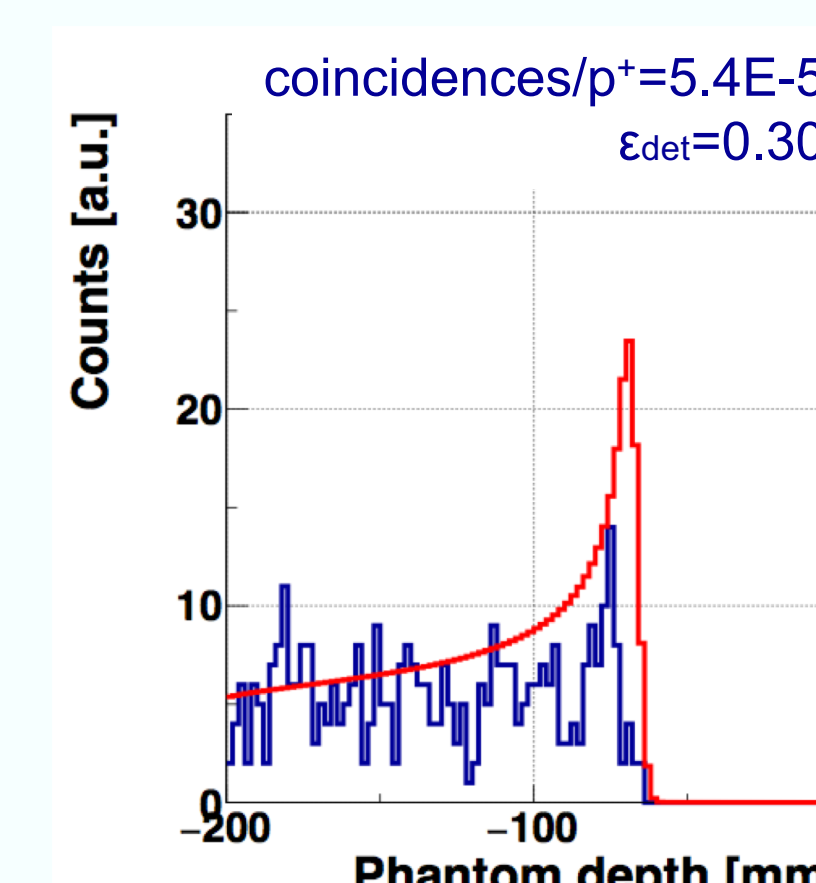


Fig. 5 (e)

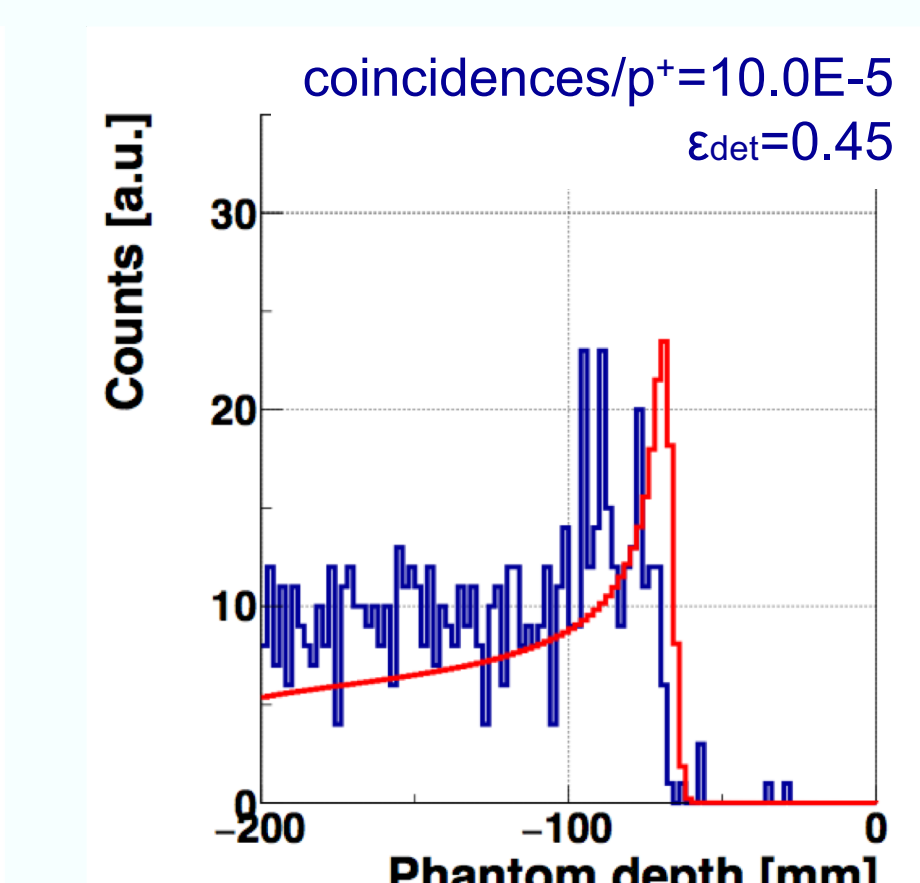


Fig. 5 (f)

### Literature:

- [1] Moskal et al. Phys. Med. Biol. 61 (2016) 2025-2047, Moskal et al. Phys. Med. Biol. 64 (2019) 055017
- [2] Rucinski et al. 2018, proceeding of IEEE Nuclear Science Symposium and Medical Imaging Conference (NSS/MIC)

Acknowledgement: Research was supported by: the National Centre for Research and Development (NCBiR), grant no. LIDER/26/0157/L-8/16/NCBR/2017, the Foundation for Polish Science (FNP) co-financed by the EU under the European Regional Development Fund, POIR.04.04.00-00-2475/16-00, TEAM/2017-4/39. MG and JB acknowledge the support of InterDokMed project no. POWR.03.02.00-00-1013/16. This research was supported in part by computing resources of ACC Cyfronet AGH. We acknowledge the support of NVIDIA Corporation with the donation of the GPU used for this research.